SmartPark Shock Absorbers for Wind Farms

G. K. Venayagamoorthy and P. Mitra

Abstract—**Vehicle-to-grid power transactions will be integrated in future smart grids. This letter presents the novel idea of utilizing plug-in vehicle parking lots (SmartParks) to reduce the shock on the transmission lines connected to a wind farm caused by drastic variations in wind-power generation and to prevent the neighboring lines from overloading. The idea is demonstrated on a power system consisting of a large wind farm and six SmartParks modeled on a real-time simulator.**

Index Terms—**Plug-in vehicles, RTDS, vehicle-to-grid (V2G), wind farm.**

I. INTRODUCTION

DUE to the intermittent nature of wind-power generation, several problems can occur in grid connected mode, including power oscillations and transmission-line power flows exceeding their limits. A wind farm with energy storage that maintains a constant power output can be used to mitigate these problems. The energy-storage unit is generally connected to the dc link in between the rotor and grid-side inverters of the doubly fed induction generator (DFIG) [1]. However, if the wind farm is large and consists of several DFIGs, the required number of energy-storage units and converters will also be large. This will increase the cost and require a complex control strategy. This letter presents the utilization of plug-in vehicle (PEV) parking lots (SmartParks) located in the vicinity of a wind farm to address this problem. The number of PEVs will increase over time, and many of them are likely to participate in vehicle-to-grid (V2G) power transactions in future smart grids as policies and business models are created [2]. Under such a scenario, it is reasonable to assume that SmartParks, used as bulk energy storage, can absorb system shocks caused by sudden fluctuations in wind speed.

II. TEST SYSTEM AND SHOCK ABSORBER

The test system (see Fig. 1) is a modified 12-bus system [3] in which one hydro unit is replaced by a 400-MW wind farm. For simplicity, the wind farm is represented by a single wind turbine with a DFIG having back-to-back pulse width modulation (PWM) converters. Data for the wind farm and the vector control strategy are mostly similar to [4]. The only difference is that a maximum power-tracking technique is used for the rotor-side converter. The system is built on a real-time digital simulator.

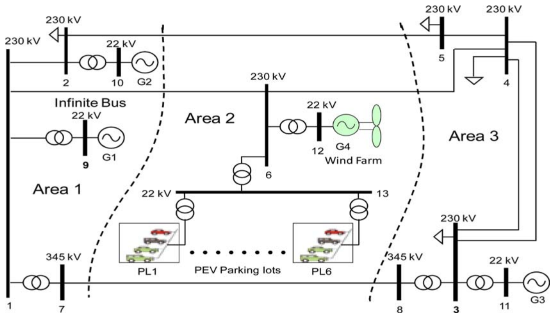

Fig. 1. Modified 12-bus power system with a wind farm and six SmartParks.

At average wind speed, Area-1 exports power to Area-2 and Area-2 exports to Area-3 through transmission lines 1–6 and 6–4, respectively. When wind speed and, subsequently, wind-farm power drop, the deficit is overcome by the infinite bus, and the power flow through lines 1–6 rises suddenly, exceeding its limit. Conversely, the power flow through lines 6–4 decreases. The opposite happens when the wind speed increases. Wind power is limited by pitch control, and due to its large time constant, power oscillations occur at the wind-farm bus and in the nearby lines. To mitigate these shocks, SmartParks are presented as shock absorbers. It is assumed that P_w, $P_{w\max}$, and $P_{w\min}$ are the average, maximum, and minimum wind-power generations, and $P_{L1\text{–}6}, P_{L1\text{–}6\max}$ and $P_{L6\text{–}4}, P_{L6\text{–}4\max}$ are the average and the maximum tolerable power flow through lines 1–6 and 6–4, respectively. For the SmartParks to behave as shock absorbers and prevent the power flows in these lines from exceeding their maximum limits, the total capacity of SmartParks is given by $P_{\mathrm{SP}1\text{–}6}$ and $P_{\mathrm{SP}6\text{–}4}$, respectively:

$$P_{\mathrm{SP}1\text{–}6} \geq (P_w - P_{w\min}) - (P_{L1\text{–}6\max} - P_{L1\text{–}6}) \qquad (1)$$

and

$$P_{\mathrm{SP}6\text{–}4} \geq (P_{w\max} - P_w) - (P_{L6\text{–}4\max} - P_{L6\text{–}4}). \qquad (2)$$

Power flows in lines 1–6 and 6–4 exceed their limits if the right-hand sides of (1) and (2) are positive. The required SmartParks' total capacity P_{SP} to satisfy (1) and (2) is

$$P_{\mathrm{SP}} = \mathrm{Max}\,(P_{\mathrm{SP}1\text{–}6}, P_{\mathrm{SP}6\text{–}4}). \qquad (3)$$

Considering P_w, $P_{w\max}$, and $P_{w\min}$ as 350, 400, and 160 MW, $P_{L1\text{–}6}$ and $P_{L1\text{–}6\max}$ as 180 and 250 MW, and $P_{L6\text{–}4}$ and $P_{L6\text{–}4\max}$ as 75 and 250 MW, respectively, from (1)–(3), P_{SP} is calculated as 120 MW (the power outputs from generators G2 and G3 are assumed constant). To achieve a realistic scenario,

Manuscript received August 17, 2010; revised February 28, 2011 and April 8, 2011; accepted May 17, 2011. Date of publication July 22, 2011; date of current version August 19, 2011. This work was supported by the National Science Foundation under Grant EFRI 0836017. Paper no. TEC-00108-2010.

The authors are with the Real-Time Power and Intelligent System Laboratory, Missouri University of Science and Technology, Rolla, MO 65409 USA (e-mail: gkumar@ieee.org; pmitra@ieee.org).

Color versions of one or more of the figures in this paper are available online at http://ieeexplore.ieee.org.

Digital Object Identifier 10.1109/TEC.2011.2159549

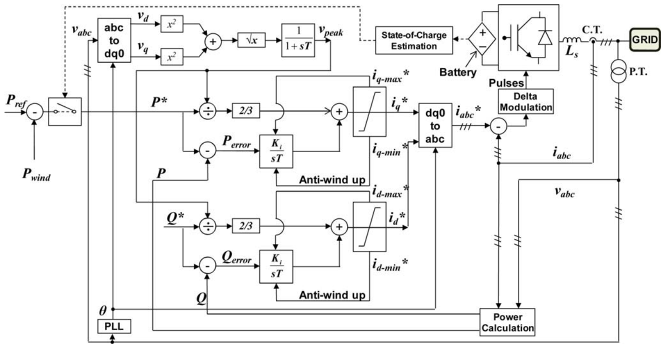

Fig. 2. Modeling and control of SmartParks as shock absorbers.

120 MW is distributed between six 20-MW SmartParks. Considering that each vehicle can supply or draw 25 kW (25% of the peak-power ratings of a standard 15.1-kW·h SAFT Li-ion battery [5]), each SmartPark must hold at least 800 vehicles, which is quite realistic for large cities. Each SmartPark is modeled as a battery with a bidirectional, three-phase inverter (see Fig. 2) connected to bus 6 through a 2.08-kV/22-kV step-up transformer (see Fig. 1). In a *d–q* reference frame, the active and reactive powers outputs of the inverter are

$$P = \left(\frac{3}{2}\right) \cdot (v_{qs} i_{qs} + v_{ds} i_{ds}) \tag{4}$$

and

$$Q = \left(\frac{3}{2}\right) \cdot (v_{qs} i_{ds} + v_{ds} i_{qs}). \tag{5}$$

In a synchronous reference frame, the peak line-to-neutral voltage is in the *q*-axis and $v_{ds} = 0$. The basis of the control is to command the currents in response to demanded power as

$$i_{qs}^* = \left(\frac{2}{3\sqrt{2}}\right) \cdot \left(\frac{P^*}{v_{\text{peak}}}\right) + \left(\frac{K_i}{s}\right) \cdot (P^* - P) \tag{6}$$

$$i_{ds}^* = \left(\frac{2}{3\sqrt{2}}\right) \cdot \left(\frac{Q^*}{v_{\text{peak}}}\right) + \left(\frac{K_i}{s}\right) \cdot (Q^* - Q). \tag{7}$$

The first components of (6) and (7) are based on (4) and (5), where v_{peak} is the filtered version of the line-to-neutral root-mean-square voltage. This creates a fast response to sudden changes in commanded power. The integral term trims out the steady-state error. A proportional-integral controller can be used to further improve inverter control. A limit is placed on the commanded current to prevent integrator windup. The commanded *q–d* currents are, then, transformed to *a–b–c* variables, where delta modulation is used for control (see Fig. 2).

To use SmartParks as shock absorbers, the average wind power is considered as the reference P_{ref}. The generated power P_{wind} is subtracted from P_{ref}, and the error is used as the active power command for the SmartParks. A state-of-charge (SOC) estimator at the battery can be used to reset the power command for the SmartParks to zero if the batteries reach their charge/discharge limits. The shock absorber's time of operation $(t_f - t_i)$ can be calculated by the following equation:

$$\int_{t_i}^{t_f} (P_{\text{wind}}(t) - P_{\text{ref}}) \cdot dt = \int_{q_i}^{q_f} v(q) \cdot dq \tag{8}$$

where q_i and q_f are the initial and the final SOC at times t_i and t_f, respectively, and $v(q)$ is the battery voltage as a function of the SOC.

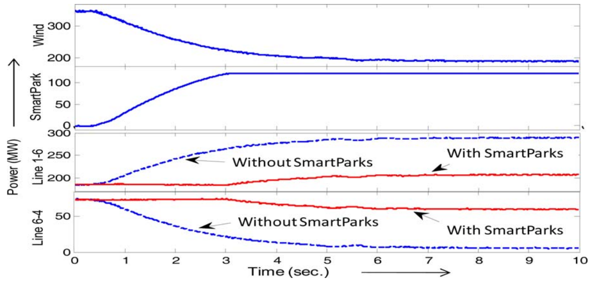

Fig. 3. Results for a drop in the wind speed from 12 to 10 m/s.

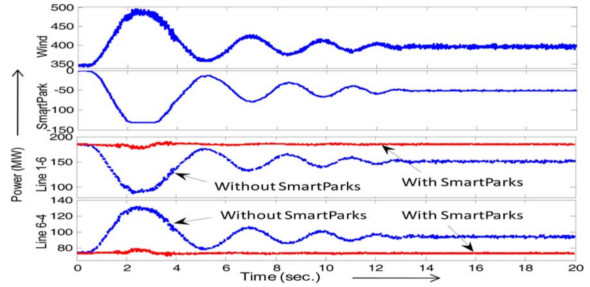

Fig. 4. Results for a rise in the wind speed from 12 to 15 m/s.

III. RESULTS AND DISCUSSIONS

With a drop in wind speed from 12 to 10 m/s (see Fig. 3), the wind farm's power drops from 350 to 200 MW. Consequently, without the shock absorber, the power through lines 1–6 rises to 290 MW, exceeding its maximum limit. With the shock absorber, however, the line's flow is maintained near 200 MW. The SmartParks supply their maximum power. In lines 6–4, the power flow is reduced by only 15 MW from its nominal value with the SmartParks. Otherwise, the reduction is close to 70 MW, and almost no power is exported to Area 3. With a rise in the wind speed from 12 to 15 m/s (see Fig. 4), and with a controlled pitch, oscillations occur in the wind farm's output and the line flows in the absence of a shock absorber. But with the shock absorber, the wind farm's output is maintained and the oscillations are absorbed. Here, "–" means the batteries are being charged.

The advantage of this type of bulk energy storage is that it is made up of smaller, distributed, portable batteries. The cost per unit is lower and the ownership is distributed. The practicality of SmartParks in grid services is addressed in [2].

IV. CONCLUSION

The application of SmartParks as shock absorbers for wind farms is presented. The shock absorbers are designed for a realistic power-system scenario, and their modeling and controls are developed and demonstrated on a real-time simulation platform. With wind-power variations, it is shown that shock absorbers maintain nearly constant line flows and prevent them from exceeding their limits. Power-system oscillations are mitigated and stability is enhanced.

REFERENCES

[1] S. Teleke, M. E. Baran, A.Q. Huang, S. Bhattacharya, and L. Anderson, "Control strategies for battery energy storage for wind farm dispatching," *IEEE Trans. Energy Convers.*, vol. 24, no. 3, pp. 725–732, Sep. 2009.

[2] A. Y. Saber and G. K. Venayagamoorthy, "Intelligent unit commitment with vehicle-to-grid – A cost-emission optimization," *J. Power Sources*, vol. 195, no. 3, pp. 898–911, 2010.

[3] S. Jiang, U. D. Annakkage, and A. M. Gole, "A platform for validation of FACTS models," *IEEE Trans. Power Delivery*, vol. 21, no. 1, pp. 484–491, Jan. 2006.

[4] W. Qiao, R. G. Harley, and G. K. Venayagamoorthy, "Coordinated reactive power control of a large wind farm and a STATCOM using heuristic dynamic programming," *IEEE Trans. Energy Convers.*, vol. 24, no. 2, pp. 493–503, Jun. 2009.

[5] M. S. Duvall, "Battery evaluation for plug-in hybrid electric vehicles," in *Proc. IEEE Vehicle Power Propulsion Conf.*, 2005. DOI: 10.1109/VPPC.2005.1554580.